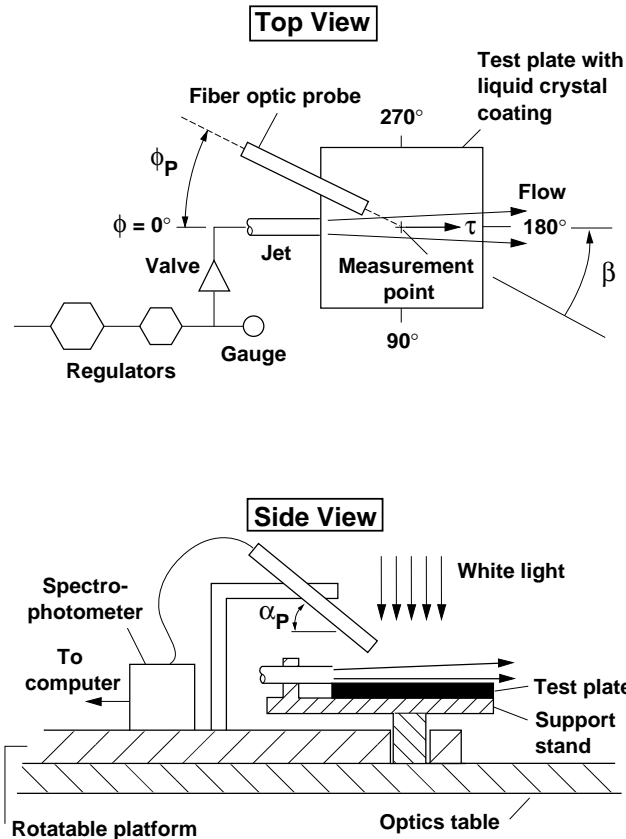# Measurement of Continuous Surface Shear Stress Vector Distributions

Lecture Two

D. C. Reda and M. C. Wilder

NASA - Ames Research Center
Moffett Field, CA

Schematic of experimental arrangement for spectrophotometer measurements of tangential jet shear field.

The experimental arrangement shown above was devised to quantify the liquid crystal color-change responses to shear illustrated in Lecture 1. A tangential jet of air (D = 0.33 in. and $250 \leq V_j \leq 750$ ft/s) was blown across a liquid crystal coated planar test surface (a 5 x 5-in. plate). The pressure difference used to drive this flow was controlled by two pressure regulators in series, and its value was indicated by a calibrated gauge. It can be shown that the pressure difference (total - static) used to drive the jet is proportional to the shear stress. Absolute shear stress values were not measured; rather, parametric values of relative surface shear stress magnitude $1 \leq \tau/\tau_r \leq 8$ were employed. A fiber optic probe at $\alpha_P = 30$ deg was used to capture light scattered from a point on the centerline of the wall jet flow. The effective sampling diameter of this sensor was order 0.10 in. The measurement point was always coincident with the center of rotation of the probe-traversing system thereby allowing the relative in-plane view angle between the shear vector and the observer (β) to be systematically varied. Note that the $\beta = 0$-deg orientation corresponds to the case where the shear vector is aligned with and directed away from the observer. Light captured by the probe was input to a spectrophotometer (Oriel Instaspec II diode array system) which dispersed it into its spectral content. Measurements of scattering intensity from the coating as a function of the wavelength of light were thus obtained over the entire visible spectrum for each τ/τ_r setting.
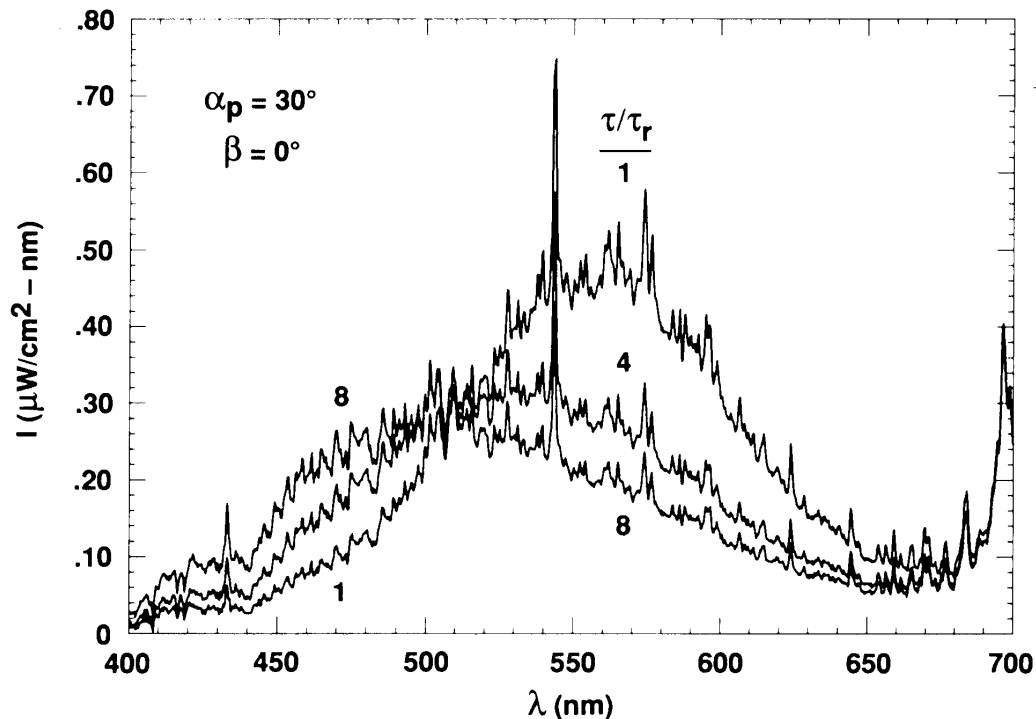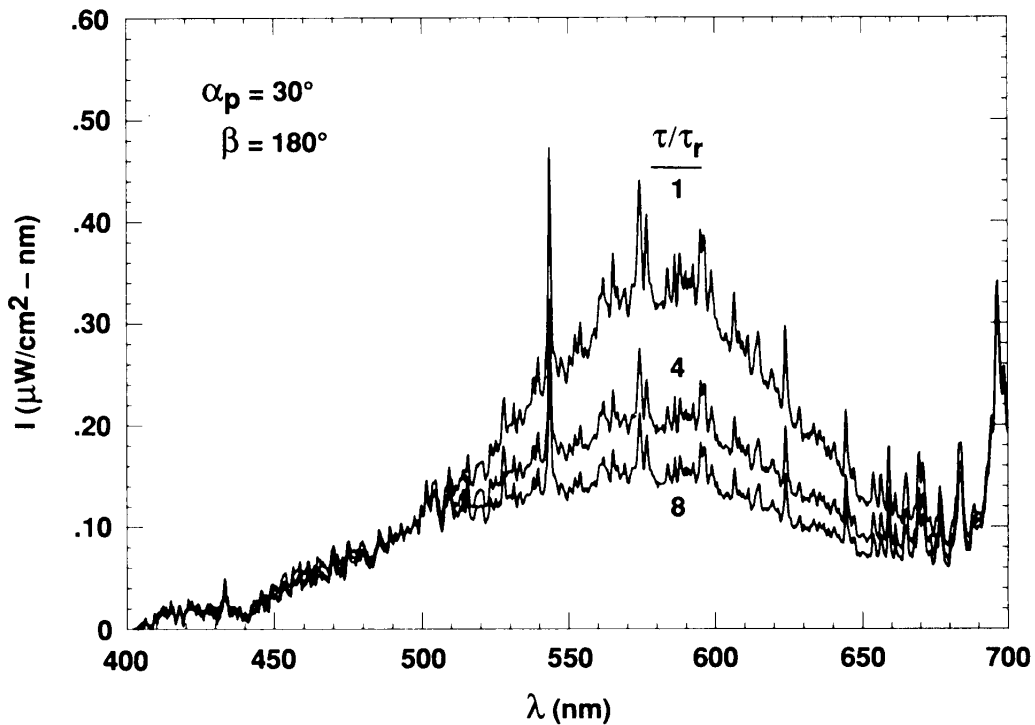
Liquid crystal coating spectra; scattering intensity vs wavelength for flow away from the observer, with relative surface shear stress magnitude as the parameter.

Spectral Measurements

Normal white light (5600 K) was supplied from a NAC Visual Systems HMI-1200 unit incorporating a 1200-W Sylvania PAR64 BriteBeam source with an ultraviolet filter and a flicker-free ballast. The intensity/wavelength distribution for this light source was shown in Lecture 1. The mean intensity level was seen to be relatively constant over the visible spectrum. The pronounced spikes are a characteristic of the light source itself and will be seen to reoccur at these fixed, discrete wavelengths in all subsequent spectra.

This figure shows measured liquid crystal coating reflected spectra for the case of flow directly away from the observer, with relative surface shear stress magnitude as the parameter. As shear magnitude was increased, the peak intensity of the scattered light was seen to decrease. More importantly, the wavelength corresponding to this peak intensity was seen to shift to lower wavelengths, indicating a shift in color from orange, through yellow and green, to blue.

Liquid crystal coating spectra; scattering intensity vs wavelength for flow toward the observer, with relative surface shear stress magnitude as the parameter.

This figure shows measured liquid crystal coating reflected spectra for the case of flow directly toward the observer, again with relative surface shear stress magnitude as the parameter. Here, in marked contrast to the results of the preceding figure, as shear magnitude was increased, the peak intensity of the scattered light decreased, but no shift in the wavelength corresponding to this peak intensity was measured, i.e., no color change occurred.
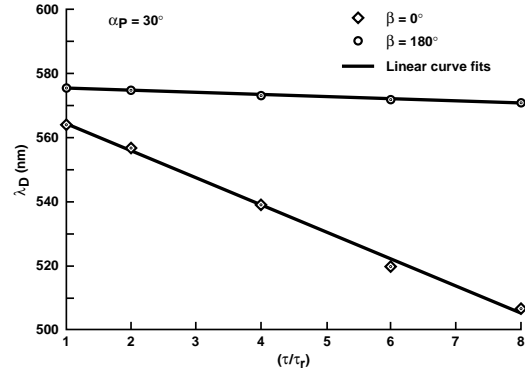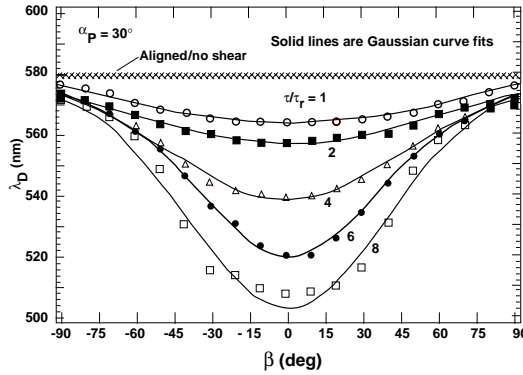
Dominant wavelength vs. relative in-plane view angle between observer and shear vector, with relative shear magnitude as the parameter.

Dominant wavelength vs. relative shear magnitude for relative in-plane view angles of 0° and 180°.

Proof-of-Concept Results

These figures summarize the present proof-of-concept measurements. The figure on the left shows an ensemble plot of λ_D vs β for data taken throughout the color-change regime ($-90 \leq \beta \leq 90$ deg) with relative surface shear stress magnitude as the parameter. Two principal results are evident: 1) for a given shear stress magnitude, the minimum dominant wavelength, i.e., the maximum color change, is measured when the shear vector is aligned with, and directed away from, the observer ($\beta = 0$ deg); and 2) for a given shear stress magnitude, changes in relative circumferential-view angle β to either side of the vector/observer aligned position result in symmetric increases in measured dominant wavelength. Furthermore, it was found that each of these measured data sets could be well fit by a Gaussian curve for $-90 \leq \beta \leq 90$ deg.

The figure on the right shows two plots of measured dominant wavelength vs relative surface shear stress magnitude. For $\beta = 0$ deg, measured color change was seen to scale linearly with increasing τ/τ_r over the entire regime tested. At shear magnitudes beyond $\tau/\tau_r = 8$, only small additional decreases in λ_D were measured, i.e., this particular liquid crystal material experiences its full-spectrum, color-change response (orange to blue) in the shear range $1 \leq \tau/\tau_r \leq 8$. In marked contrast, the $\beta = 180$ deg data set shows no color-change response over the same τ/τ_r range.

These measurements are entirely consistent with the visual observations noted in Lecture 1.
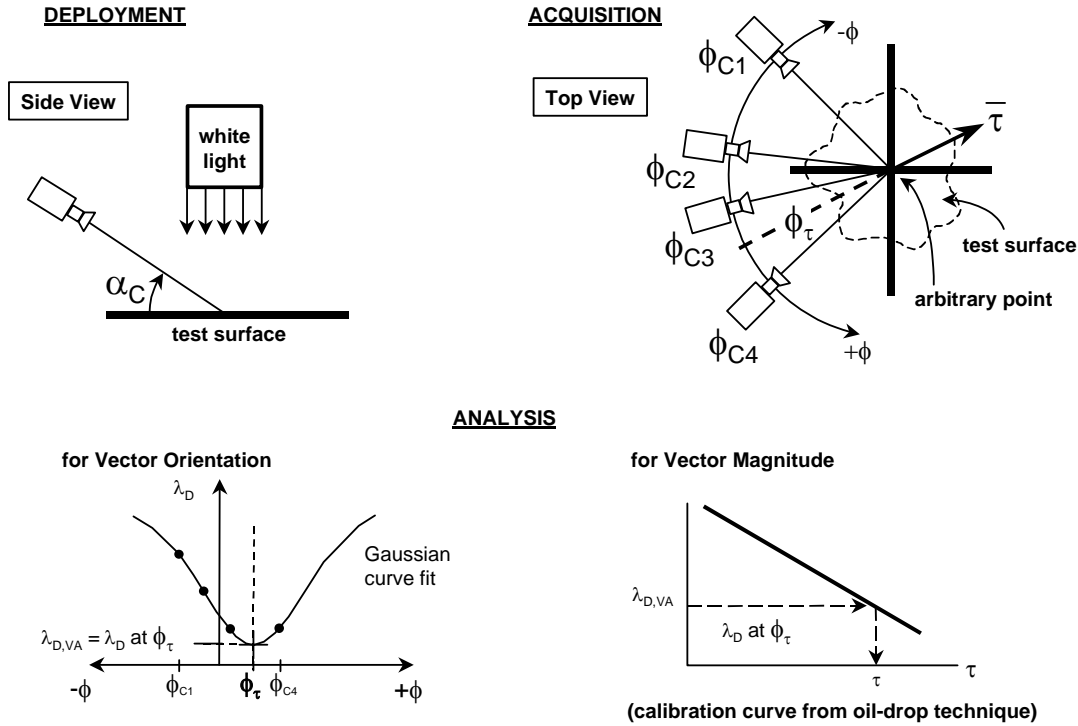
Schematic of full-surface shear stress vector measurement methodology.

The data presented in the previous two figures were used to formulate the full-surface shear stress vector measurement method shown schematically above. The coated test surface is illuminated from the normal direction with white light and the camera is positioned at an above-plane view angle (α_C) of approximately 30 deg. For quantitative measurements, images of the SSLCC color-change response to the shear field are recorded from multiple in-plane view angles encompassing all shear vector directions to be measured (shown here as ϕ_{C1} to ϕ_{C4}). As shown earlier, the color-change response to a constant shear stress vector is a Gaussian function of the relative in-plane view angle between the observer and the vector orientation. Therefore, the shear vector orientation can be determined at each physical point on the test surface by fitting a Gaussian curve to the variation in measured color (λ_D) with changing in-plane view angle (ϕ_C) at that point on the surface. In theory, a minimum of four images is required to obtain the Gaussian curve fit, but in practice this number is generally increased consistent with optical access. The in-plane angle corresponding to the maximum color-change value of the curve-fit determines the vector orientation (ϕ_τ), and the value of the vector-aligned color ($\lambda_{D,VA}$) is then related to the shear magnitude (τ) via a calibration curve acquired using conventional point-measurement techniques, for example, the fringe-imaging skin friction, or "oil-drop," technique discussed elsewhere in this Lecture Series.

Imaging Concerns

When quantitative measurements are required, a 3-CCD, co-site sampling, RGB (red, green, and blue) video camera is preferred. This type of camera, which is typically used in medical imaging applications, records the light intensity of the NTSC (National Television Systems Committee) standard RGB components of the scattered light using three CCD chips. Features that compensate for the nonlinear brightness response of the human eye, such as automatic gain and non-unity gamma, should be deactivated. Each color component is digitized using a frame grabber. An 8-bit per channel (24-bit color) digitizer provides better that 1 nm color resolution, while coating-to-coating repeatability is typically 2 to 3 nm.

The color measurements are rendered illuminant invariant through a linear color correction that references all measurements to the CIE (Commission Internationale d'Eclairage) Illuminant C. Color is determined from the measured RGB intensities by calculating hue, an intensity-invariant measure of color which can be directly related to dominant wavelength through the CIE colorimetric system.

Two imaging concerns need to be addressed: reflected glare and potential saturation of one or more of the color signals. Reflected glare can be minimized by adjusting the relative angular orientation of two linear polarizing filters: one placed on the camera lens, and the second placed between the light and the coated test surface. The circularly polarized light scattered from the SSLCC is unaltered by this approach. To overcome the second concern, images can be recorded at two or more exposure settings, and a composite image can be formed using only the correctly exposed pixels from each image. This technique is possible since color (dominant wavelength) is independent of intensity.

Calibration and Data Analysis Concerns

  In-situ calibration of the SSLCC is optimally achieved after the unscaled data set, comprised of a vector-aligned color (proportional to shear magnitude) and a vector orientation at every grid point on the surface, has been acquired. In this manner, the point-measurement method of choice (e.g., the oil-drop technique) can be employed at precise locations to encompass the complete range of vector-aligned colors (shear magnitudes) encountered in the flow under study.

  Calibration of SSLCC materials in a mechanical shearing apparatus such as a rotating-disc or rotating-shaft device is not recommended. The no-slip boundary condition coupled with the relative motion between the moving and fixed surfaces forces a velocity distribution to occur within the liquid crystal material. This flow situation alters the liquid crystal molecular arrangement and thus its color-change response as compared to the application of aerodynamic shear to the exposed surface of a non-flowing SSLCC.

  The signal-to-noise ratio of images can be improved by frame-averaging several images (for steady-flow applications) and/or by spatially filtering the images. Spatial filtering involves replacing the RGB values of each pixel with the average of its neighboring pixels, and sacrifices spatial resolution in favor of increased signal-to-noise ratio. Typically a 3x3 or 5x5 pixel neighborhood is used.

  The color (λ_D) measurements used in the Gaussian curve-fit portion of the analysis must be obtained at the same physical location on the surface for each in-plane view angle. This requires mapping the color images onto a common grid on the physical surface through the principles of photogrammetry.

  SSLCC vector measurement resolution and accuracy issues were discussed in detail by Wilder & Reda (6) and Reda *et al*. (8). Uncertainties of 2 to 4% in shear vector magnitude and less than 1 deg in shear vector orientation have been attained for absolute magnitudes in the range of 5 to 50 Pa (0.1 to 1 psf).
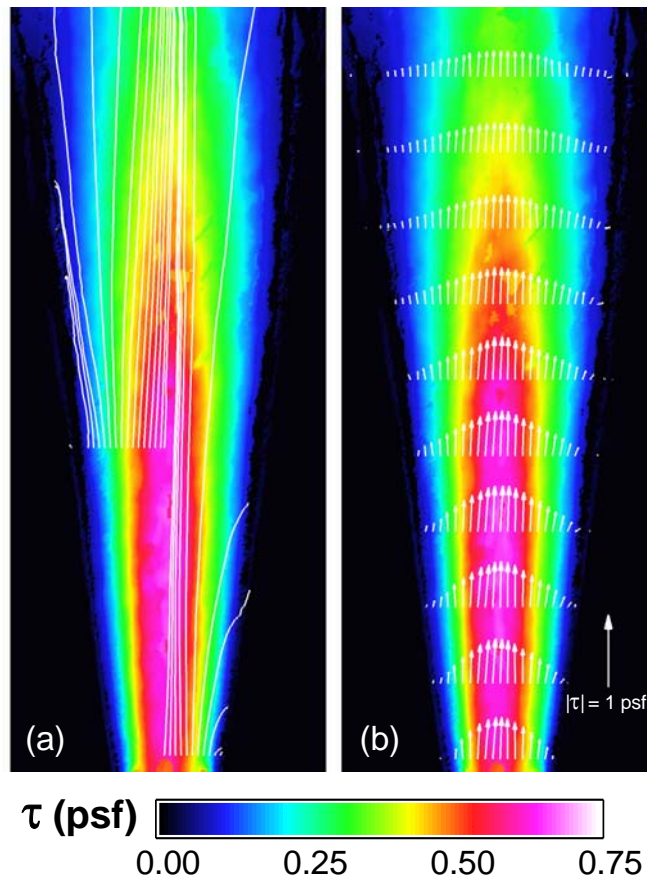
Measured surface shear stress vector field beneath tangential jet where color contours show vector magnitudes: (a) vector orientations shown by streaklines originating from X/D = 5 and 10; (b) vector cross-stream profiles starting at X/D = 5, every ΔX/D = 1.23.

The SSLCC vector measurement methodology was first applied to measure the shear stress vector distribution on a planar surface beneath an axisymmetric, turbulent, wall-jet flow. Results are summarized below.
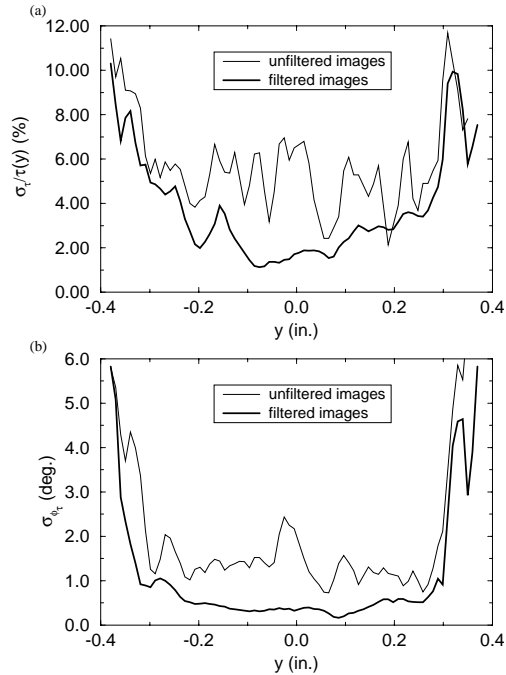
This figure shows two representations of the wall-jet-induced shear stress vector distribution as measured by the SSLCC technique. This data set was generated by analyzing seven low-pass-filtered color images, and it contains approximately 10^5 measured vector values.

Both images shown above use false color levels to represent the shear stress magnitude distribution. Vector orientations are illustrated by streaklines on the left and by vector profiles on the right. These streaklines are drawn tangent to the local shear stress vector at every point along their trajectories. The vector profiles are drawn every 1.23D (every 40th profile) starting at the axial location of X/D = 5. For clarity, only every fourth vector is shown in each profile. As can be seen, maximum shear stress magnitudes occurred along the wall jet centerline, decreasing laterally toward the outer edges of the shear field.
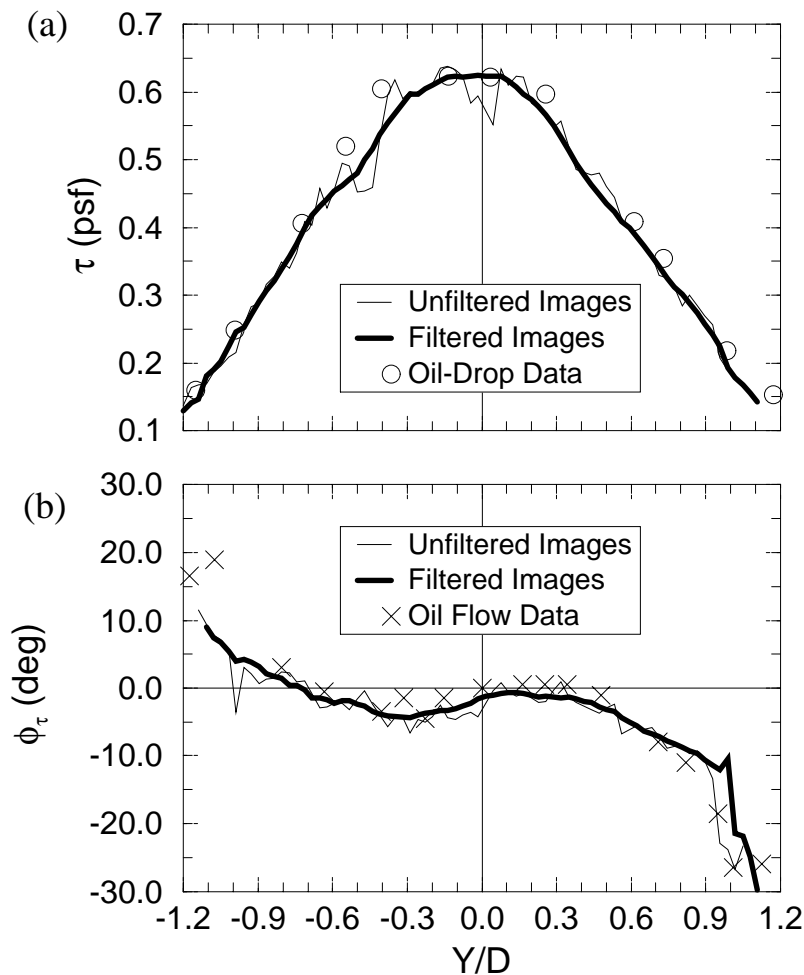
Cross-stream profiles of shear vector field beneath tangential jet at
X/D = 9: (a) magnitude vs. oil-drop data; (b) orientation vs. oil-flow
data.

Quantitative comparisons with point measurements taken across the wall jet shear field at a single axial station (X/D = 9) are shown above. The point measurements of magnitude were made using the FISF or oil-drop method. Vector directions across this axial station were determined by measuring the tangent angle of the streaklines generated in a separate oil-flow visualization experiment. These comparisons show good overall agreement between the SSLCC measurements and the point measurements across the entire shear field. Note that the vector directions across the core region of the shear field all fell between ±10 deg and that the SSLCC technique measured these directions to within 1-2 deg even though no color images were recorded between $\phi_c = 0$ and ±10 deg. This is a clear indication of the robustness of the variation of λ_D vs ϕ and the Gaussian curvefitting procedure used in the SSLCC methodology.

(a)

12.00

10.00

8.00

$\sigma_\tau/\tau(y)$ (%)

6.00

4.00

2.00

0.00

-0.4   -0.2   0.0   0.2   0.4

y (in.)

unfiltered images
filtered images

(b)

6.0

5.0

4.0

σ_{ϕ_τ} (deg.)

3.0

2.0

1.0

0.0

-0.4   -0.2   0.0   0.2   0.4

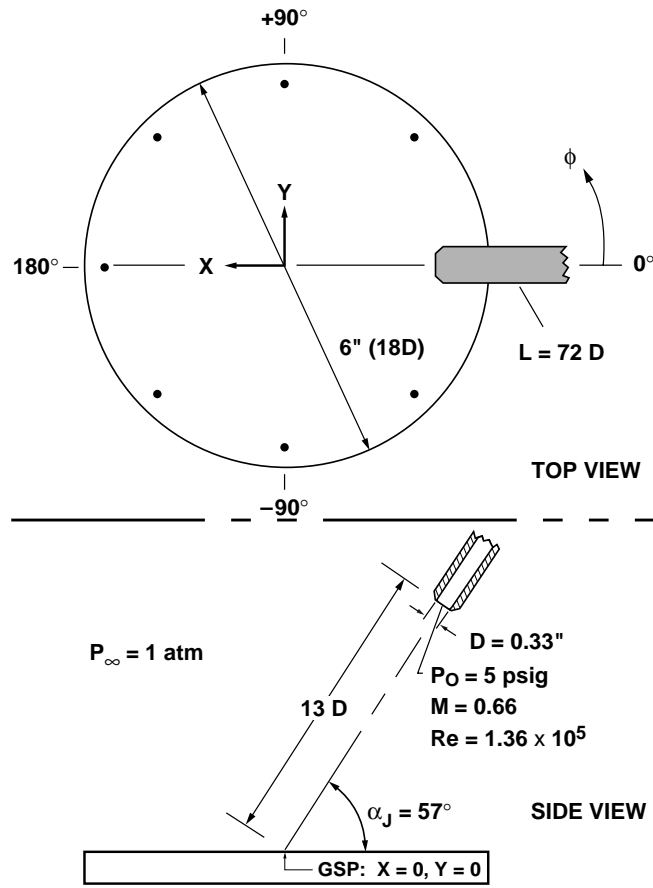y (in.)

unfiltered images
filtered images

Cross-stream profiles of measured standard deviations for wall-jet shear field: (a) shear vector magnitude uncertainty, non-dimensionalized by local shear magnitude (percent) and (b) shear vector orientation uncertainty (deg).

These figures show the standard deviation profiles for τ and ϕ_τ at the X/D = 9 axial station. At each point along the cross-cut profile, the mean values and the standard deviations were determined using a 3 x 9 pixel region centered around each point. Comparisons between the data values (τ and ϕ_τ) at each point and mean values showed that the shear field was sufficiently constant across this 3 x 9 pixel region for the standard deviations to reasonably estimate the measurement uncertainties.

Across the main extent of the shear field, -0.3 in. < y < 0.3 in., the standard deviations calculated from the unfiltered data were in the range of 4 to 6% of the local shear magnitude, with corresponding uncertainties of 1 to 2 deg in ϕ_τ. Standard deviations calculated from the filtered data sets were about half these levels, namely 2 to 4% of local shear magnitude and less than 1 deg in vector orientation.

At the edges of the shear field, for |y| > 0.3 in. (|y/D| > 0.9), the local shear magnitude decreases significantly and the ability of the SSLCC technique to resolve vector orientations, and thus vector magnitudes, is degraded. In this low-shear limit, standard deviations of the orientation data were as high as 6 deg with corresponding shear magnitude uncertainties on the order of 10%.

This low-shear limitation is defined in the present methodology by four factors: 1) the low-shear response of the SSLCC mixture; 2) the resolution of the imaging system; 3) the total number of hue images acquired and the $\Delta\phi_C$ spacing between images; and 4) the analysis methods applied to these color images.

+90°

φ

Y

180° ⎯ X ⎯ 0°

6" (18D)

L = 72 D

TOP VIEW

−90°

D = 0.33"

P_∞ = 1 atm

P_O = 5 psig

13 D

M = 0.66

Re = 1.36 x 10^5

α_J = 57°   **SIDE VIEW**

GSP: X = 0, Y = 0

Schematic of Experimental Arrangement for Measurement of Shear Vector Distribution Beneath an Inclined, Impinging Jet.

The SSLCC methodology was also applied to measure the shear stress vector distribution on a planar surface beneath an inclined, axisymmetric, turbulent impinging jet.

A twenty-frame-average RGB image of the complete test surface was recorded from each of fifteen ϕ_C orientations over the arc $0 \leq \phi_C \leq 180$ deg. Due to the widely varying RGB intensities experienced within each such color image, all ϕ_C images were recorded at two or more exposure settings then mathematically combined to form a single, composite image wherein each pixel was correctly exposed. All such composite images were low-pass filtered using a 5x5 pixel mask and converted from RGB to an HSI color space.

Taking advantage of the symmetry of the flow field, the time-averaged, filtered hue images for $0 \leq \phi_C \leq 180$ deg were mirror-imaged across the plane of symmetry (the X axis) to form a complete $0 \leq \phi_C \leq 360$ deg image set. These hue images were then subjected to the image processing and data analysis procedure outlined earlier. The resulting surface shear stress vector distribution is shown on the next page.
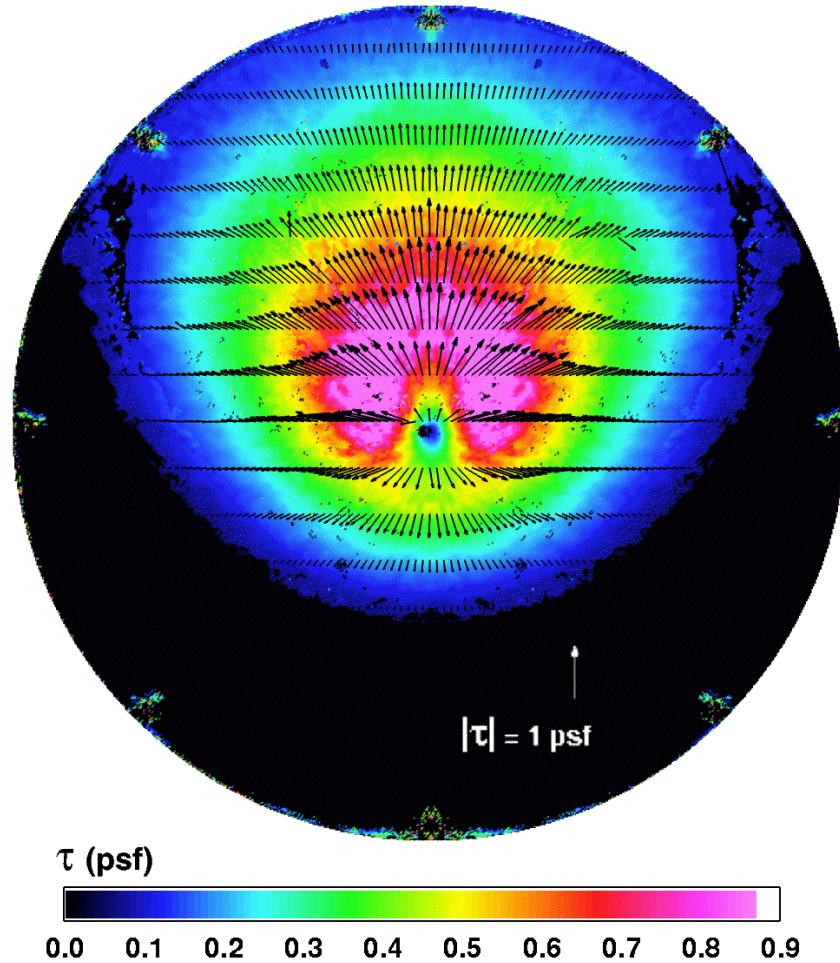
Measured Surface Shear Stress Vector Field Beneath Inclined, Impinging Jet: Color Contours Show Vector Magnitudes and Vector Cross-Cut Profiles Every $\Delta X/D = 1$ Show Vector Orientations.

This measured data set contains approximately 2×10^5 non-zero vectors, one at every point on a surface grid whose resolution is 100x100 points per square inch. False color levels are used to represent shear stress magnitudes. Black regions represent the absence of a vector value due either to thresholding at the lowest non-zero calibration point or to the failure to attain an acceptable Gaussian curve fit to the color vs. ϕ data set at a particular surface grid point. Vector orientations are illustrated by the vector cross-cut profiles drawn every $\Delta X/D = \pm 1$ starting at the Y axis; for clarity, only every fifth vector, spaced at $\Delta Y/D = 0.15$, is shown in each profile.

A local minimum in shear magnitude was seen to occur in the immediate vicinity of the geometric stagnation point (GSP). Shear magnitude increased rapidly in all directions emanating from the stagnation zone as the inclined-jet flow turned to align itself with the plate surface, then accelerated outwards. Peak shear stresses were measured in all radial directions within 2D of the GSP.
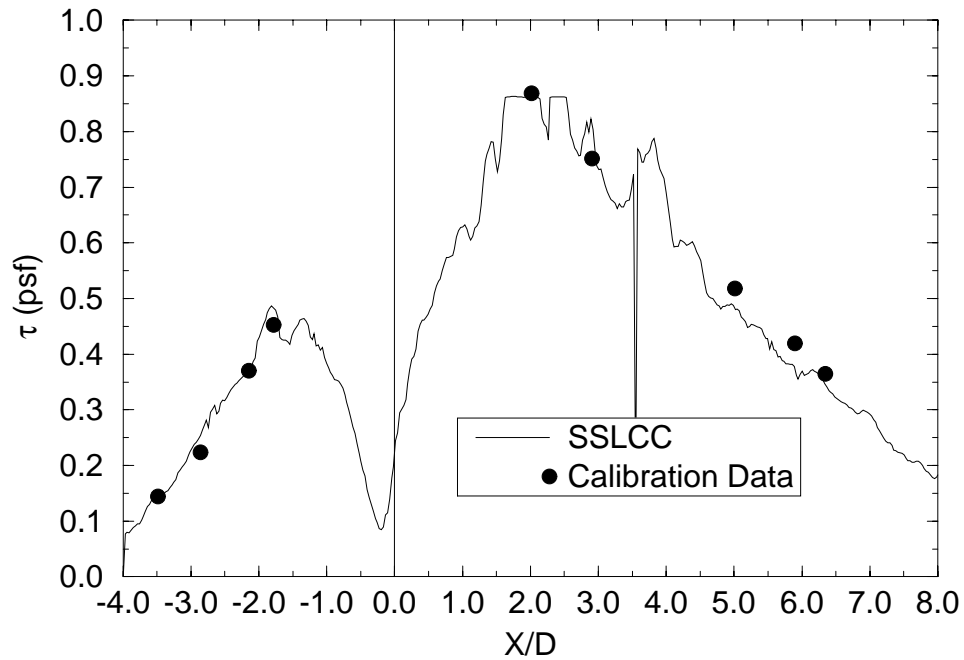
Shear Magnitude Distribution Along X Axis For Inclined, Impinging Jet.

This figure shows the shear magnitude distribution on the X axis, along with the oil-drop data used for calibration purposes. A shear minimum occurred just to the negative X side of the GSP. Due to thresholding applied in the SSLCC method, and/or possibly to unsteadiness observed in this region, a non-zero value of the time-averaged shear magnitude was measured at the stagnation point.
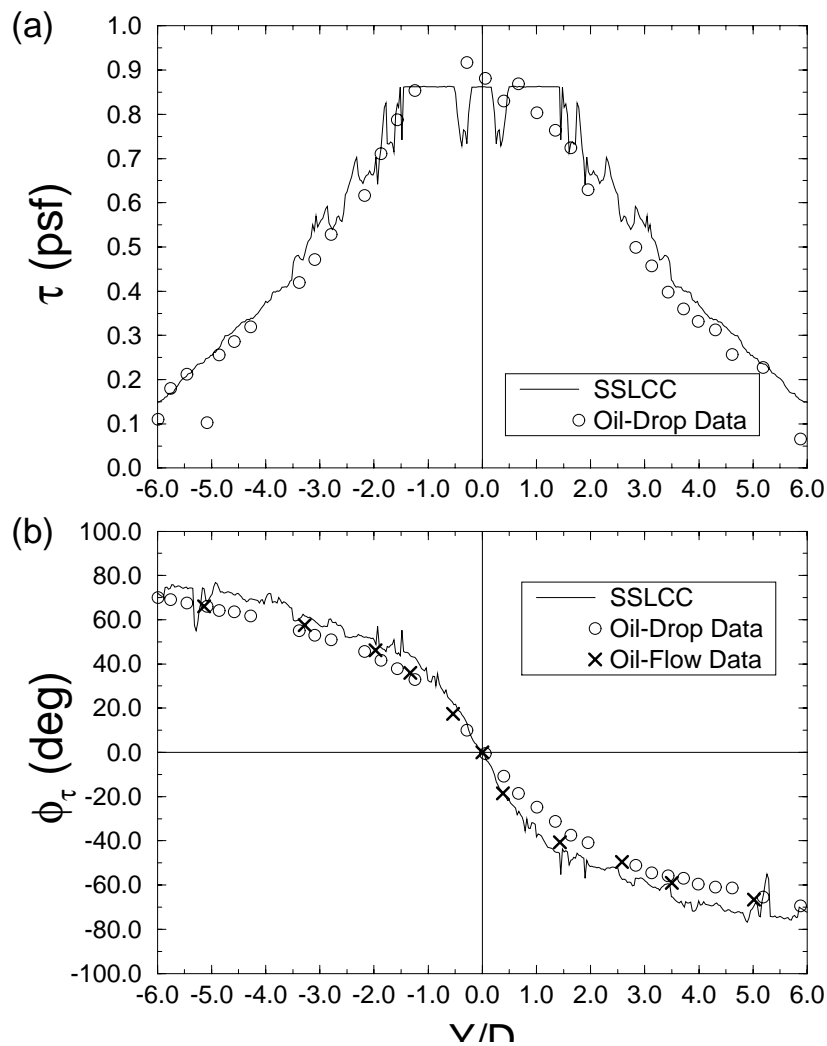
Cross-stream profiles of shear vector field beneath inclined, impinging
jet at X/D = 2: (a) magnitude; (b) orientation.

These figures show continuous measurements from the SSLCC method versus
point measurements from the oil-drop technique as acquired on a transverse cross-cut at
X/D = 2. None of the oil-drop data shown here were used in calibration. Very good
overall agreement was noted between shear vector magnitudes and shear vector
orientations measured by these two methodologies. Calibration data for $\tau > 0.87$ psf
(41.7 Pa) were not available, hence the SSLCC magnitude data are clipped near the
centerline at this station.

These results provided the first demonstration of the capability of the SSLCC
method to reliably measure continuous shear stress vector distributions on planar surfaces
were shear vectors of all possible orientations were present.

Summary

Based on present results, it has been shown that the shear-sensitive liquid crystal coating technique can be utilized to obtain areal measurements of surface shear stress vector distributions on planar surfaces with accuracies equivalent to conventional point-measurement techniques.

This full-surface technique requires an image-based instrumentation system that incorporates white-light illumination normal to the coated test surface and allows for oblique observations with an RGB color camera. Multiple in-plane view angles encompassing the shear vector directions to be measured are required while maintaining the same above-plane view angle (~30 deg) for each image.

The approach includes an illuminant-invariant color calibration procedure previously validated in research using thermochromic liquid crystal coatings for measurements of surface temperature distributions. A single calibration of color vs shear magnitude is required for the specific arrangement wherein the calibration shear vector is aligned with and directed away from the camera. Existing point-measurement techniques, such as oil-drop interferometry, can be utilized for this purpose.

Once color and shear calibrations have been accomplished, full-surface color images are acquired as a function of in-plane view angle. For each physical point on the test surface, a Gaussian curve is fit to the dominant wavelength vs in-plane view angle data. The in-plane view angle corresponding to the minimum dominant wavelength value of the curve fit determines the vector orientation. This minimum dominant wavelength value is then input to the vector-aligned dominant wavelength vs shear magnitude calibration to determine the vector magnitude. This data analysis procedure is repeated for all surface points to determine the complete shear vector field.

Measurements of surface shear stress vector distributions beneath highly three-dimensional flows, including flows with regions of reversal, are now possible on planar surfaces, limited solely by optical access.

References

1. Reda, D.C. and Wilder, M.C., "Shear-Sensitive Liquid Crystal Coating Method Applied Through Transparent Test Surfaces," <u>AIAA Journal</u>, Vol. 39, No. 1, 2001, pp. 195-197

2. Mehta, R. D., Bell, J. H., Reda, D. C., Wilder, M. C., Zilliac, G. G., and Driver, D.M., "Pressure and Shear Sensitive Coatings," <u>Flow Visualization: Techniques and Examples</u>, Imperial College Press, London, 2000, pp.169-203

3. Reda, D.C. and Wilder, M.C., "The Shear-Sensitive Liquid Crystal Coating Method," <u>Sensors: the Journal of Applied Sensing Technology</u>, Vol. 15, No. 10, 1998, pp. 38-48

4. Reda, D.C. and Wilder, M.C., "Quantitative and Qualitative Aspects of the Shear-Sensitive Liquid Crystal Coating Method," ICAS 98-3.3.2, Proceedings, 21st Congress of the International Council of the Aeronautical Sciences, Melbourne, Australia, September 1998

5. Reda, D.C., Wilder, M.C., Mehta, R., and Zilliac, G., "Measurement of Continuous Pressure and Shear Distributions Using Coating and Imaging Techniques," <u>AIAA Journal</u>, Vol. 36, 1998, pp. 895-899

6. Wilder, M.C. and Reda, D.C., "Uncertainty Analysis of the Liquid Crystal Coating Shear Vector Measurement Technique," AIAA 98-2717, 20th Advanced Measurement and Ground Testing Technology Conference, Albuquerque, NM, June 1998

7. Reda, D.C. and Wilder, M.C., "Visualization and Measurement of Surface Shear Stress Vector Distributions Using Liquid Crystal Coatings," AGARD CP-601, Advanced Aerodynamic Measurement Technology Conference, Seattle, WA, September 1997, pp. 26-1 to 26-9

8. Reda, D.C., Wilder, M.C., Farina, D.J., and Zilliac, G., "New Methodology for the Measurement of Surface Shear Stress Vector Distributions," <u>AIAA Journal</u>, Vol. 35, 1997, pp. 608-614

9. Reda, D.C., Wilder, M.C., and Crowder, J.P., "Simultaneous, Full-Surface Visualizations of Transition and Separation Using Liquid Crystal Coatings," <u>AIAA Journal</u>, Vol. 35, 1997, pp. 615-616

10. Reda, D.C. and Muratore, J.J., Jr., "Measurement of Surface Shear Stress Vectors Using Liquid Crystal Coatings," <u>AIAA Journal</u>, Vol. 32, 1994, pp. 1576-1582